Toroidal rotation braking with low *n* external perturbation field on JET

Y. Sun[1], Y. Liang[1], H. R. Koslowski[1], S. Jachmich[2], A. Alfier[3], O. Asunta[4], G. Corrigan[5], C. Giroud[5], M. P. Gryaznevich[5], D. Harting[1], T. Hender[5], E. Nardon[5], V. Naulin[6], V. Parail[5], T. Tala[7], C. Wiegmann[1], S. Wiesen[1] and JET-EFDA contributors*

JET-EFDA, Culham Science Centre, Abingdon, OX14 3DB, UK.
[1] *Institute for Energy Research – Plasma Physics, Forschungszentrum Jülich, Association EURATOM-FZJ, Trilateral Euregio Cluster, 52425 Jülich, Germany*
[2] *Association EURATOM-Belgian State, Koninklijke Militaire School-Ecole Royale Militaire, B-1000 Brussels, Belgium*
[3] *Associazione EURATOM-ENEA sulla Fusione, Consorzio RFX Padova, Italy*
[4] *Association EURATOM-Tekes, Helsinki University of Technology, P.O. Box 4100 FI-02015 TKK, Finland*
[5] *EURATOM-UKAEA Fusion Association, Culham Science Centre, Abingdon, OX14 3DB, UK*
[6] *Association EURATOM–Risø National Laboratory, OPL-128 Risø, DK-4000 Roskilde, Denmark*
[7] *Association EURATOM-Tekes, VTT, P.O. Box 1000, FIN-02044 VTT, Finland*

1. **Introduction.** Toroidal plasma rotation in a tokamak is of great importance for plasma confinement, because of its stabilization effects on Resistive Wall Modes (RWMs) [1] and Neoclassical Tearing Modes (NTMs) [2] and its shear stabilization effect on turbulence [3]. External magnetic field perturbation have been frequently used to actively control or mitigate Edge Localized Modes (ELMs) on many tokamaks [4,5,6]. It was also used to feedback control RWMs [7]. However, both resonant [8] and non-resonant [9,10] component of the perturbation field can influence the plasma rotation. Non-resonant magnetic braking effects have been reported from many tokamaks recently [11,12,13].

The paper is organized as follows: The torque induced by the *n*=1 **E**rror **F**ield **C**orrection **C**oils (EFCCs) current, T_{EFCC}, is determined by momentum transport analysis using the JETTO code [14] in Sec. 2. The **N**eoclassical **T**oroidal **V**iscosity (NTV) torque [9,15] is calculated and compared with T_{EFCC} in Sec. 3, followed by the summary of the main results in Sec. 4.

2. **Determination of the torque induced by the magnetic perturbation field on JET.** It is found that the toroidal plasma rotation velocity, measured by Charge eXchange Recombination Spectroscopy (CXRS), shows a 50% reduction with a *n*=1 perturbation field amplitude which is only about 0.1-0.2% of the toroidal field strength as shown in Figure 1.

The angular momentum transport equation in the JETTO code can be written in

$$\frac{\partial}{\partial t}\left(\left\langle R^2 \right\rangle \sum_{ions} n_j m_j \omega \right) + fA \frac{1}{\rho}\frac{\partial}{\partial \rho}\left[\rho \frac{\left\langle R^2 \right\rangle}{fA} \sum_{ions} \left(m_j \omega \Gamma_j^p + \Gamma_j^\omega \right) \right] = T^\phi \qquad (1)$$

where R is the major radius, $\langle ... \rangle$ denotes the flux surface average, $\sum_{ions}$ denotes the sum over all ion species, n_j and m_j are the density and mass of the ion species, respectively, $\omega = V_\Phi / R$ is the angular rotation frequency and V_Φ is the torodial rotation velocity, $f = RB_\Phi$ and B_Φ is the toroidal magnetic field, $A = \langle 1/R^2 \rangle$ is a geometrical quantity, ρ is the flux-surface label related to the toroidal flux, T^ϕ is the source torque, Γ_j^p and Γ_j^ω are the ion particle flux and angular momentum flux, respectively, defined as $\Gamma_j^p = -\left(D_j \left\langle |\nabla\rho|^2 \right\rangle \frac{\partial n_j}{\partial \rho} + \left\langle |\nabla\rho| \right\rangle V_{p,j} n_j \right)$, and

* See the Appendix of F. Romanelli et al., Proceedings of the 22nd IAEA Fusion Energy Conference, Geneva, Switzerland, 2008

$\Gamma_j^{\omega} = -m_j n_j \left(\chi_M \left\langle |\nabla\rho|^2 \right\rangle \frac{\partial\omega}{\partial\rho} + \left\langle |\nabla\rho| \right\rangle V_{inwm}\omega \right)$, D_j and $V_{p,j}$ are the ion particle diffusion coefficient and pinch velocity profiles, respectively, χ_M and V_{inwm} are momentum diffusion coefficient and pinch velocity profiles, respectively. At each time step, $\gamma \equiv \rho_i\omega \equiv \sum_{ions} n_j m_j \omega$ is solved in the JETTO code. The particle flux is neglected in the following analysis.

The χ_M and V_{inwm} profiles are obtained by fitting the observed velocity evolution after the switch-off of the EFCC current by using Eq. (1). At this stage, the only source term is the NBI torque, which is calculated by the PENCIL code [16]. The polynomial function is used as base function, $\chi_M \equiv \sum_{n=0}^{N} \alpha_n \rho^n$; $V_{inwm} \equiv \sum_{m=0}^{M} \beta_m \rho^m$, here α, β are the unknown free parameters to be fitted, N and M are the orders of the polynomial base function.

The torque induced by the EFCC current at its current flat top phase, T_{EFCC}, is calculated by solving Eq. 1 with other terms determined. Figure 2 shows the obtained T_{EFCC} (solid line) profile by using the χ_M and V_{inwm} profiles fitted from different orders of polynomial base functions. Two of them do not consider the pinch velocity in momentum flux with N=4 and N=6, and the other two consider the pinch velocity with M=N=4 and M=N=6. The obtained torque is not very sensitive to the selected set of base function, because it is mainly determined by the total momentum flux during the EFCC current flat top phase. To separate the effects of χ_M and V_{inwm} is beyond the discussion in this paper.

The obtained torque at the plasma central region is about half of the NBI torque. The obtained T_{EFCC} has a global profile. The maximum torque is in the plasma central region, while it is found to be near the plasma edge on NSTX [11] and DIII-D [12], both using a higher *n* perturbation field. The *dL/dt* (circles + dashed line), where *L* is the angular momentum at the time just after the switch-off of the EFCC current, is also shown in Figure 2. The profile is similar to the obtained torque profile but difference about 40-50% in absolute values.

With the assumption that $T_{EFCC} \propto I_{EFCC}^2$, the simulation of the momentum transport equation can well reproduce the observed evolution of the plasma rotation as shown in Figure 3.

3. **Comparison with NTV torque.** The toroidal symmetry breaking, induced by the non-resonant magnetic perturbation field, will cause a nonambipolar radial particle flux and hence the NTV, which can dissipate the plasma momentum.

According to the NTV theory [9,15], the NTV torque in different collisionless regimes from the ions (the ions viscosity is $(m_i/m_e)^{1/2}$ times larger than the electron viscosity) can be rewritten in

$$T_{NTV} = \tau_{NTV,i}^{-1} \left\langle R^2 \right\rangle \left(\gamma - k_{c,i}\gamma_{NC0} \right) \qquad (2)$$

here $\tau_{NTV,i}^{-1} \approx \begin{cases} -1.23R_0^2 \left\langle \frac{1}{R^2} \right\rangle q^2 \frac{\omega_{ti}^2}{\nu_i} I_\lambda & \left(1/\nu, \left(q\omega_E < \nu/\varepsilon < \sqrt{\varepsilon}\omega_t\right)\right) \\ -0.13R_0^2 \left\langle \frac{1}{R^2} \right\rangle \frac{\nu_i \omega_{ti}^2}{\omega_E^{\,2}} G_\lambda & \left(\nu, \left(\nu/\varepsilon \le q\omega_E\right)\right) \\ -0.064R_0^2 \left\langle \frac{1}{R^2} \right\rangle \left[\ln\left(64q\varepsilon\omega_E/\nu_i\right)\right]^{1/2} \frac{q^2\omega_{ti}^2\sqrt{\nu_i}}{\left(|q\omega_E|\right)^{3/2}} H_\lambda & (\nu, bdy) \end{cases}$, $k_{c,i} \approx \begin{cases} 3.54 & (1/\nu) \\ 0.92 & (\nu) \\ 1.53 & (\nu, bdy) \end{cases}$,

$\omega_{ti} = v_{ti} / R_0 q$ is the transit frequency and $v_{ti} = (2T_i / m)^{1/2}$ is the thermal velocity, ν_i is ion collisionality, ω_E is the $\vec{E} \times \vec{B}$ drift frequency, I_λ (defined in [9]), G_λ (defined in [15]) and $H_\lambda = \left\{ \sum_n \sqrt{n} \left(\alpha_{bn}^2 + \beta_{bn}^2 \right) \right\}$ are the pitch angle integrations (α_{bn}, β_{bn} are defined in [15]), γ_{NC0} is defined as $\gamma_{NC0} \equiv \rho_i \frac{V_{NC0}}{R} = \rho_i \frac{cq}{e_i \rho B_0} \frac{dT_i}{d\rho}$, and $V_{NC} \equiv k_{c,i} V_{NC0}$ is the so called neoclassical velocity, $k_{c,i}$ is the coefficient of the neoclassical velocity, ν, bdy is the boundary layer contribution in the ν regime .

The vacuum field approximation is used in the NTV torque calculation. The calculated NTV torque is shown in Figure 4. The triangles are the NTV torque in the $1/\nu$ regime, the diamonds are that in the ν regime and the circles are that from the boundary layer contribution in the ν regime. In the ν regime, the boundary layer contribution is the dominant component as pointed out by Shaing [15]. Therefore, the original NTV torque in ν regime without boundary layer contribution can be neglected. The calculated NTV torque profile in the 1/ν regime agrees with the profile of T_{EFCC}, although its absolute value is a factor of 2 larger. The NTV torque in the ν regime from the boundary layer contribution is comparable to the observed T_{EFCC}.

4. **Summary.** The experimentally measured torque profile of the perturbation field induced by the *n*=1 EFCC field, T_{EFCC}, is determined by momentum transport analysis using the JETTO code. The NBI torque is calculated by the PENCIL code. The perpendicular diffusion coefficient and pinch velocity profile are determined by fitting the evolution of the velocity after the switch-off of EFCC current.

The T_{EFCC} has a global profile. The maximum torque is in the plasma central region, which is different from the observations on NSTX and DIII-D with higher n perturbation field. This torque is not localized at a certain rational surface and the velocity evolution is obviously different from that in the mode locking phase as also observed on NSTX.

With the vacuum field approximation, the NTV torque in the collisionless regime is calculated and compared with the observed T_{EFCC}. The calculated NTV torque profile in the 1/ν regime agrees with the profile of T_{EFCC}, although its absolute value is a factor of 2 larger. The NTV torque in the ν regime from the boundary layer contribution is comparable to the measured torque. Therefore, the NTV torque is in the same order as the observed T_{EFCC}. The NTV torque is a good candidate to explain the non-resonant magnetic braking observed on JET with *n*=1 perturbation field.

Acknowledgement. The authors would like to acknowledge helpful discussions with K. C. Shaing, Y. Liu, D. Howell, and V. D. Pustovitov. This work, supported by the European Communities under the contract of Association between EURATOM and Belgian State, was carried out within the framework of the European Fusion development Agreement. The views and opinions expressed herein do not necessarily reflect those of the European Commission.

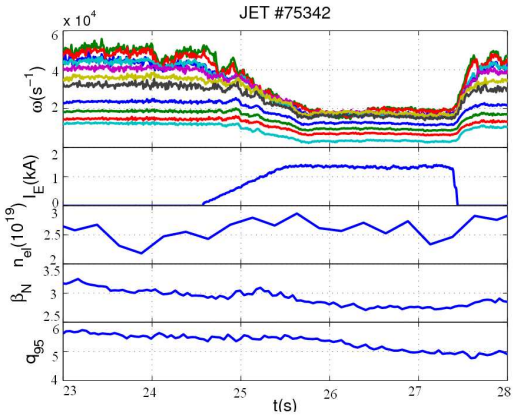

Figure1. From top to bottom, the plasma angular rotation frequency at different radii, the EFCC current I_{EFCC}, the plasma density, normalized β and q_{95} for JET pulse 75342.

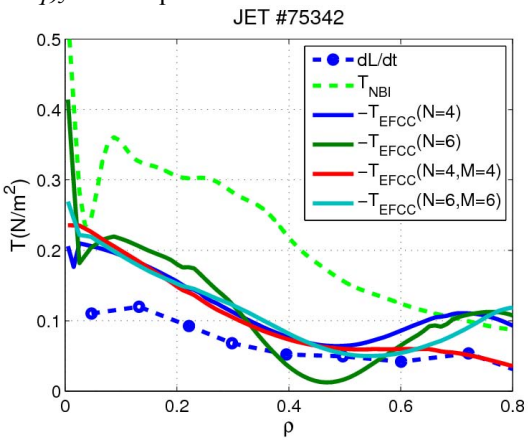

Figure 2. The obtained T_{EFCC} (solid line, times -1) profile by using the χ_M and V_{inwm} profiles fitted from different orders of polynomial base functions, the NBI torque (dashed line) and *dL/dt* (circles + dashed line) at the time just after the switch-off of the EFCC current.

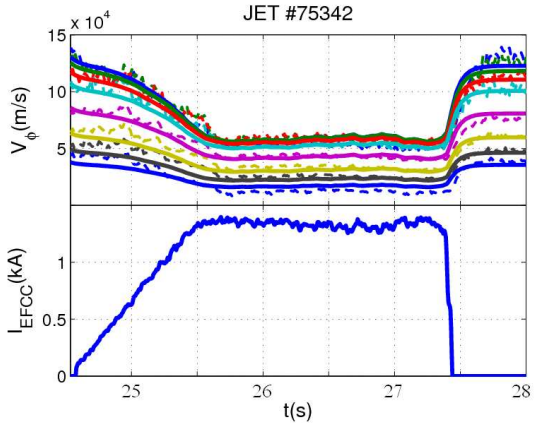

Figure 3. Comparison of the temporal evolution of the plasma velocity (top) from the experimental observation (star dashed line) and simulation (solid line). The bottom shows the time trace of the EFCC current.

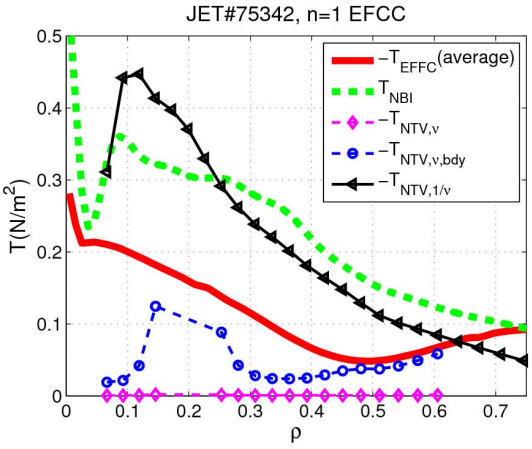

Figure 4. Comparison of the NTV torque (the triangles are the NTV torque in the $1/\nu$ regime, the diamonds are that in the ν regime, the circles are the boundary layer contribution in the ν regime) with T_{EFCC} (solid line, averaged over the four profiles in Figure 2).

[1] E. J. Strait et al., Phy. Rev. Lett. **74**,2483 (1995)
[2] R. Buttery et al., Phys. Plasmas **15**, 056115 (2008)
[3] K. H. Burrell, Science **281**, 1816 (1998)
[4] Y. Liang et al., Phy. Rev. Lett. **98**, 265004 (2007)
[5] T. Evans et al., Phys. Rev. Lett. **92**, 235003 (2004)
[6] S. J. Fielding et al., Europhys. Conf. Abstr. **25**A, 1825 (2001)
[7] Strait E.J. et al., Phys. Plasmas **11**, 2505 (2004)
[8] R. Fitzpatrick, Phys. Plasmas **5**, 3325(1998)
[9] K. C. Shaing, Phys. Plasmas **10**, 1443(2003)
[10] A. J. Cole et al., Phys. Plasmas **15**, 056102 (2008)
[11] W. Zhu et al., Phy. Rev. Lett. **96**, 225002 (2006)
[12] A. M. Garofalo et al., Phy. Rev. Lett. **101**, 195005 (2008)
[13] Y. Liang et al, 22nd IAEA Fusion Energy Conference, October 13-18, 2008, Geneva, EX/4-2
[14] G. Cenacchi and A. Taroni, (1988) "JETTO: A Free-Boundary Plasma Transport Code (Basic Version)", JET Report JET-IR(88)03
[15] K. C. Shaing, Phys. Plasmas **15**, 082506 (2008)
[16]C. D. Challis et al., Nucl. Fusion **29** 563 (1989)